A Nonlinear Back-stepping Controller of DC-DC Non Inverting Buck-Boost Converter for Maximizing Photovoltaic Power Extraction

Okba Boutebba
Dept.of Electronics
Power electronics and industrial control laboratory (LEPCI)
Sétif, Algeria
boutebbaokba@univ-setif.dz

Samia Semcheddine
Dept.of Electronics
Power electronics and industrial control laboratory (LEPCI)
Sétif, Algeria
samia.semchedine@univ-setif.dz

Fateh Krim
Dept.of Electronics
Power electronics and industrial control laboratory (LEPCI)
Sétif, Algeria
krim_f@ieee.org

Fabio Corti
Dept. of Information Engineering
Via Santa Marta 3 I-50138
Florence, Italy
fabio.corti@unifi.it

Alberto Reatti
Dept. of Information Engineering
Via Santa Marta 3 I-50138
Florence, Italy
alberto.reatti@unifi.it

Francesco Grasso
Dept. of Information Engineering
Via Santa Marta 3 I-50138
Florence, Italy
francesco.grasso@unifi.it

***Abstract*— In this paper the integration of the application of the Back-Stepping Control (BSC) strategy for the Maximum Power Point Tracking (MPPT) of photovoltaic (PV) systems is presented. The output voltage regulation and the MPPT control strategy is applied to a DC-DC Non-Inverting Buck Boost (NIBB). The robust and non-linear BSC is based on Lyapunov function for ensuring the local stability of the system. Further on, the basic idea of this later is to synthesize a recursive way control law step by step. Simulations are performed to validate the control strategy and analyze the performance. The obtained results show that the proposed solution, compared with the well-known classical PI controller, exhibits lower transient overshoot, lower tracking error and fast response when solar irradiation and cell temperature occur.**

***Keywords—Non-inverting buck-boost, back-stepping control, Photovoltaic, Maximum Power Point Tracking* (MPPT).**

I. INTRODUCTION

Nowadays, the use of renewable energies have significant increased as solution to reduce the pollution emissions at expense of energy production by fossil fuel. Anyway, the transition from fossil fuel electric production to renewable energies is a complex task [1]. More and more attention has been made from industries and academia to improve the efficiency of the chain for the energy production [2].

One of the most used renewable energy sources is the photovoltaic (PV). After a first diffusion of large photovoltaic generation plants, in the last few years the number of small power size PV system has been increasing considerably. Thus, this technology allows to distributed generation. The main benefit coming from a distributed energy production is the increment of system reliability due to the possibility to localize the impact of failure on the area of the fault reducing the number of users affected. Others benefits are an higher grid flexibility and a drastically reduction of the power losses during the transmission and distribution of the energy with a consequently increment of the system efficiency.

Independently from the power rating of the PV system, they are characterized from a single operating point able to provide to the load the maximum power. This point is called Maximum Power Point (MPP). The locus of this point has a non-linear variance under both solar radiation and cells temperature. For this reason, this paper proposes a technique able to track the MPP.

The DC-DC converter used to manage the power generated from the PV panel is the NIBB [3-4]. Then, the control strategy allows to adapt the duty cycle of the switching devices in order to track the MPP and therefore ensure the extraction of the maximum power from the panel [5].

Several MPPT control strategies have been proposed ove the year in literature. The most used are the P&O (perturb and observe) [6-7], incremental conductance [2], [7], predictive model based approaches[8-9], SMC (sliding mode control) [10-13], FL (fuzzy) and ANN (artificial neural network methods) [14-16].

This paper proposes and examines a non-linear back-stepping controller for the regulation of the duty cycle of an NIBB converter. The duty cycle is changed depending on the environmental conditions and on the desired output voltage. A P&O algorithm delivers the output reference voltage of the PV array to reach the MPP speedily. The results shows that the stability and the MPP is maintained under any environmental condition's changes thanks to the improvement of the robustness through the Lyapunov's law.

The paper is organized in the following sections. In Section II the electrical model of the photovoltaic system is the described in detail. In Section III the proposed BSC algorithm is discussed with special focus on the practical implementation for PV devices. In the fourth and fifth sections, the Simulink comparison versus the classic P&O/PI controller, will be presented. Conclusion and final remarks will close the paper.

978-1-7281-7455-6/20/$31.00 ©2020 IEEE

II. OVRALL SYSTEM CONFIGURATION

Fig. 1. shows the architecture of the proposed system.

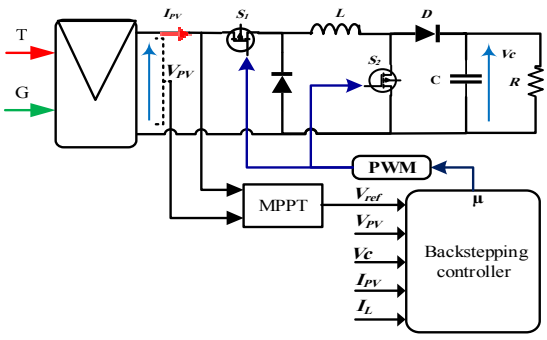

Fig. 1. Architecture of the stand-alone photovoltaic system.

The proposed control solution is made up from two steps. The control algorithm is based on a a P&O which generates the reference voltage V_{ref} and improved by a BSC controlled to enforce the Vpv to track $Vref$ and to provide the duty ratio μ in order to achieve an optimal exploitation of the generator photovoltaic under any environmental condition's changes.

A. PV panel modeling

The equation which describe the behavior of the PV panel depending on the number of cells connected in series or in parallel is [14-16]:

$$\mathrm{I_{PV}} = \mathrm{I_{Ph}} - \mathrm{I_0}\left[\exp\left(\frac{\mathrm{V_{PV}} + \mathrm{Rs}\ \mathrm{I_{PV}}}{\alpha\, Vt}\right) - 1\right] - \left(\frac{V_{PV} + Rs\ I_{PV}}{R_{Sh}}\right) \quad (1)$$

Where I_{ph} is the photo-generated current :

$$I_{Ph} = \left(I_{PV\_n} + Ki\ \Delta T\right)\frac{G}{G_n} \quad (2)$$

where I_{PV_n} is the current generated by the light, Ki is current coefficient, $\Delta T = T - Tn$ (T and Tn are the actual and nominal temperatures, respectively), G and G_n are respectively the actual and nominal solar irradiation. The thermal voltage V_t is

$$Vt = \frac{Ns\ K\ T}{q} \quad (3)$$

where Ns *is* the number of series cells, K is Boltzmann's constant and q is the electrical charge, Kv is the voltage coefficient. The dark saturation current is:

$$I_0 = \frac{I_{sc\_n} + K\ \Delta T}{\exp\left(V_{oc\_n} + \frac{Kv\ \Delta T}{\alpha\, Vt}\right)} \quad (4)$$

where I_{sc_n} and V_{oc_n}, are the short-circuit current and open circuit voltage respectively, α is the diode ideality factor.

Being the PV array made up from many panels connected in series and in parallel, the model of the whole array is

$$I_{PV} = N_{PP}\ I_{ph} - N_{pp}\ I_0\left[\exp\left(\frac{N_{SS}\ V_{PV} + Rs\left(\frac{N_{SS}}{N_{PP}}\right)}{\alpha\, Vt\ N_{SS}}\right) - 1\right] - \left(\frac{N_{SS}\ V_{PV} + Rs\ I_{PV}\left(\frac{N_{SS}}{N_{PP}}\right)}{R_{sh}\left(\frac{N_{SS}}{N_{PP}}\right)}\right) \quad (5)$$

where *Nss, Npp* are the number of PV panels connected in series and parallel respectively.

B. Non inverting buck-boost converter modeling

The DC-DC Non-inverting buck-boost converter, also known as "four switch buck boost converter" [3], [4] is used for tracking the maximum power point of the PV panels, and feeding the load by operating the switch $\boldsymbol{S_1}$ and $\boldsymbol{S_2}$**.** The dynamic model of the NIBB converter in term of duty cycle "$\boldsymbol{\mu}$" is given by using the averaging method presented in [18]:

$$\begin{cases} \dot{x}_1 = \dfrac{I_{PV}}{C_1} - \mu\dfrac{x_2}{C_1} \\ \dot{x}_2 = -\dfrac{x_3}{L} + \mu\left(\dfrac{x_1 + x_3}{L}\right) \\ \dot{x}_3 = \dfrac{x_2}{C_2} - \dfrac{x_3}{RC_2} - \mu\dfrac{x_2}{C_2} \end{cases} \quad (6)$$

where $x = (x_1, x_2, x_3)^T = (V_{PV}, I_L, V_S)^T$, represents the state vector and $\mu = (0,1)$ is the duty cycle of the signal control considered as input variable.

III. BSC DESGIN

To obtain the optimal reference voltage, the P&O algorithm is used to extract the maximum energy from the photovoltaic generator. A non-linear BSC aims to track this reference voltage of the photovoltaic generator by regulating the duty cycle μ of the NIBB [17]. BSC being a recursive control law, the calculation of the control law must be done in several steps.

Step 1: Find, a virtual control law

To start the controller design it is necessary to define the error signal, which is defined as the difference between the actual voltage V_{PV} and the desired voltage:

$$e_1 = x_1 - x_{1-ref} \quad (7)$$

where $x_{1\text{-}ref}$, is the voltage reference generated by the P&O algorithm. By forcing the voltage error to ($\boldsymbol{e_1 = 0}$), the desired performance can be achieved.

The derivative of the tracking error is written using equation (7) as follows

$$\dot{e}_1 = \frac{I_{PV}}{C_1} - \frac{x_2}{C_1}\mu - \dot{x}_{1-ref} \quad (8)$$

We consider the function of lyapunov to be as follows

$$V_1 = \frac{1}{2}e_1^2 \quad (9)$$

To verify and assure the asymptotic stability, the lyapunov's function must be positive $V_1 > 0$ and its time derivative must be certainly negative. $\dot{V_1} < 0$.

Taking the derivative with respect to time of (9), we get

$$\dot{V_1} = e_1 \dot{e_1} \tag{10}$$

$$\dot{V_1} = e_1 \left[\frac{I_{PV}}{C_1} - \frac{x_2}{C_1}\mu - \dot{x}_{1\_ref} \right] \tag{11}$$

From (11) in order that the derivative of lyapunov function is negative, verification is necessary

$$\frac{I_{PV}}{C_1} - \frac{x_2}{C_1}\mu - \dot{x}_{1\_ref} = -K_1 e_1 \tag{12}$$

At this point, the virtual control law can be written as follows

$$x_2 = \frac{C_1}{\mu}\left[K_1 e_1 + \frac{I_{PV}}{C_1} - \dot{x}_{1\_ref} \right] \tag{13}$$

Taking the value of x_2 from (13), (11) becomes

$$\dot{V_1} = -K_1 e_1^2 \tag{14}$$

The derivative of V_1 is definitively negative if K_1 is positive, moreover, equation (10) must be verified.

Then the function of stabilization β defined by

$$\beta = \frac{C_1}{\mu}\left[K_1 e_1 + \frac{I_{PV}}{C_1} - \dot{x}_{1\_ref} \right] \tag{25}$$

Therefore, the original system asymptotic stability calculated by (6) is achieved..

Step 2: Original Control Input μ

The second error variable, which represent the difference between the state variable $x_2 = I_L$ and its desired value β, is set by

$$e_2 = x_2 - \beta \tag{16}$$

By differentiating (16), equation (8) will become

$$\dot{e_1} = -K_1 e_1 - \frac{e_2}{C_1}\mu \tag{17}$$

The derivative of e_2 can be defined as:

$$\dot{e_2} = \dot{x}_2 - \dot{\beta} \tag{18}$$

Therefore,

$$\dot{e_2} = \dot{x}_2 - \frac{C_1}{\mu}\left[-K_1^2 e_1 - \frac{K_1 . e_2}{C_1}\mu + \frac{\dot{I}_{PV}}{C_1} - \ddot{x}_{1\_ref} \right] + \frac{\dot{\mu}}{\mu}\beta \tag{19}$$

The derivate of the composite Lyapunov function Vt has to be negative for every x_1 and x_2 to allow the achievement of the asymptotic stability and the convergence of the errors $(e_1 , e_2) = (0,0)$ [16], [19]

$$Vt = V_1 + \frac{1}{2}e_2^2 \tag{20}$$

The Vt derivative is

$$\dot{Vt} = \dot{V_1} + e_2 \dot{e_2} \tag{21}$$

$$\dot{Vt} = -K_1 e_1^2 + e_2\left(\dot{e_2} - \frac{e_1}{C_1}\mu \right) \tag{22}$$

To ensure that the value of Vt derivative's negative, must be verified

$$\left(\dot{e_2} - \frac{e_1}{C_1}\mu \right) = -K_2 e_2 \tag{23}$$

So $\dot{V_t}$ becomes:

$$\dot{Vt} = -K_1 e_1^2 - K_2 e_2^2 \tag{24}$$

Where

$$\dot{\mu} = \frac{1}{\beta}\left[\mu . e_2 (-K_2 - K_1) - e_1\left(K_1^2 C_1 - \mu^2 \frac{1}{C_1} \right) + \mu \frac{x_3}{L} \right] + \frac{1}{\beta}\left[\dot{I}_{PV} - C_1 \ddot{x}_{1\_ref} - \mu^2\left(\frac{x_1 + x_3}{L} \right) \right] \tag{25}$$

IV. SIMULATION RESULTS OF BSC

The PV system shown in Figure 1 is simulated in MATLAB Simulink® environment. As case study, a PV array made up from four panels, connected two in parallel and two in series is assumed. The main characteristics of the system are shown in Table I.In this scenario (A), the temperature T is fixed at T= 25 °C and the solar insolation G is then subject to changes according to the profile given in Figure 2. The irradiance stays at 1000 W/m² for 0.5s and then decreases linearly for another 0.5s until it reaches 250 W/m². Thereafter, there are four successive step changes, in which the irradiance shows variations in steps (250-750) W/m², (750-500) W/m², (500-750) W/m² and (750-250) W/m². Finally, the irradiation level gradually increases from 250 W/m² up to 1000 W/m².As clearly demonstrated by the simulations performed for each irradiation level, as shown in Figure 3 the proposed BSC successfully tracks the $V_{PV\text{-}ref}$ reference voltage. The performance of this latter is then confirmed.

A. Scinario 1 :at various levels of irradiance G (W/m²)

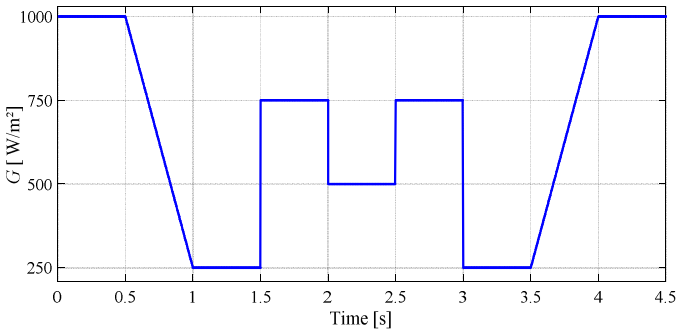

Fig. 2. Irradiance.

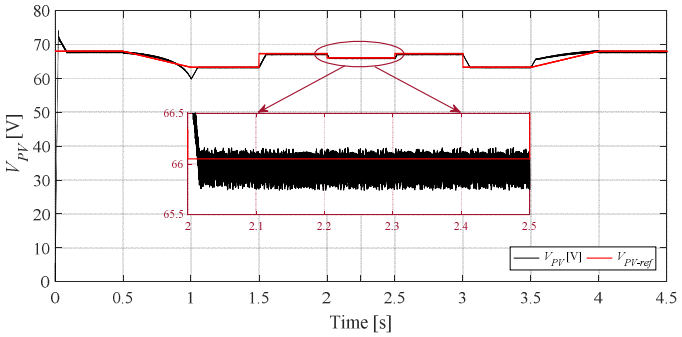

Fig. 3. Simulated PV voltage with P&O/BSC for different values of irradiation.

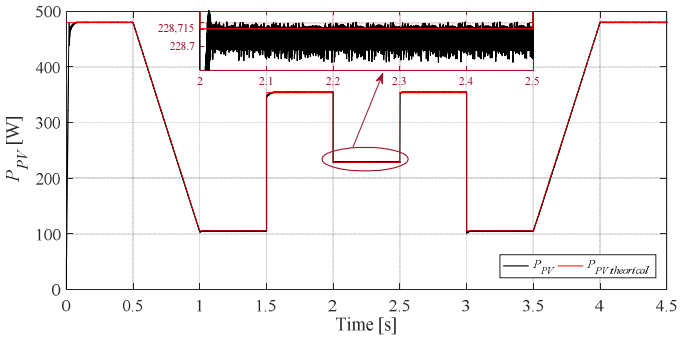

Fig. 4. Simulated PV power with P&O/BSC (black) and $P_{PV\text{-theorical}}$ (red) for different values of solar irradiation.

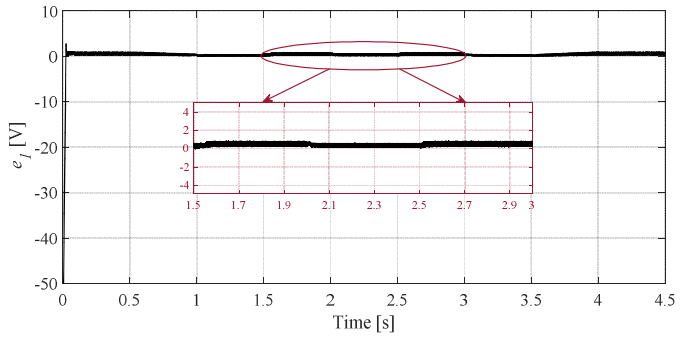

Fig. 5. Error signal e_1.

B. Scinario 2: at various levels of temperature T (°C)

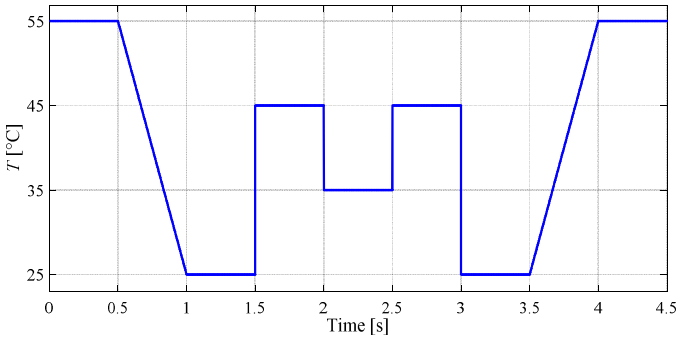

Fig. 6. Temperature variations.

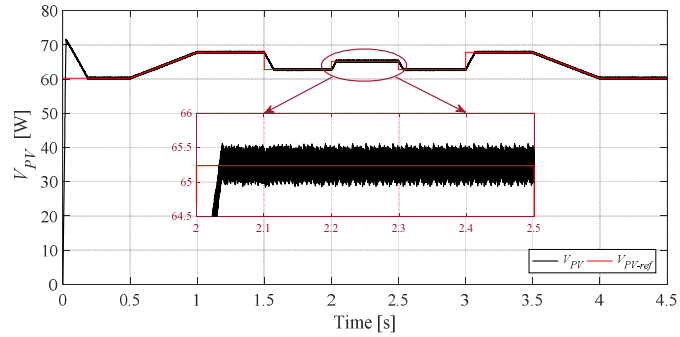

Fig. 7. Simulated PV voltage with P&O/BSC for different values of temperature

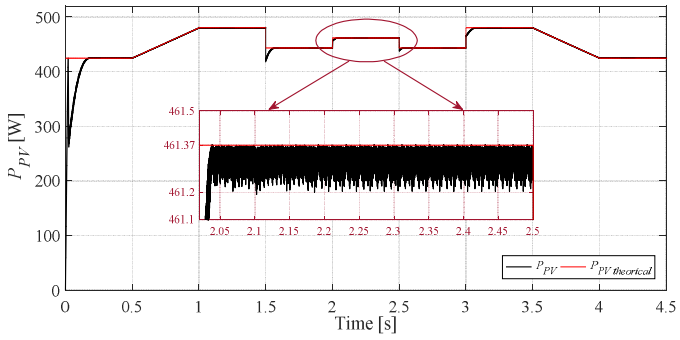

Fig. 8. Simulated PV power with P&O/BSC (black) and $P_{PV\text{-theorical}}$ (red) for different values of temperature.

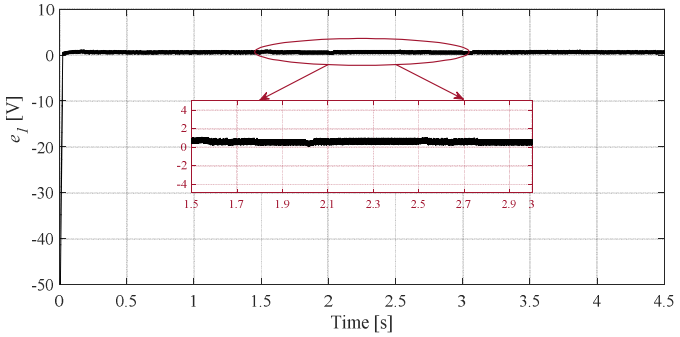

Fig. 9. Error signal e_1 .

Figure 4. shows the results obtained for the overall power of the PV generator with the BSC controller. The proposed controlled ensure good performance under any variations of irradiation. It can be seen that the proposed controller has excellent and very well performance at any change in irradiation level.

In Figure 5 it is shown that the error e_1 signal converge to zero.

V. Simulation with PI Controller and Comparison

To demonstrate the BSC's efficiency, the results obtained in this paper are compared with those that the classical PI controller achieves. The comparison is based on simulations which use the same changes in temperature and irradiation as those used for the BSC in the previous section. The PWM frequency is the same of the sampling time .

A. Comparison under varying irradiance

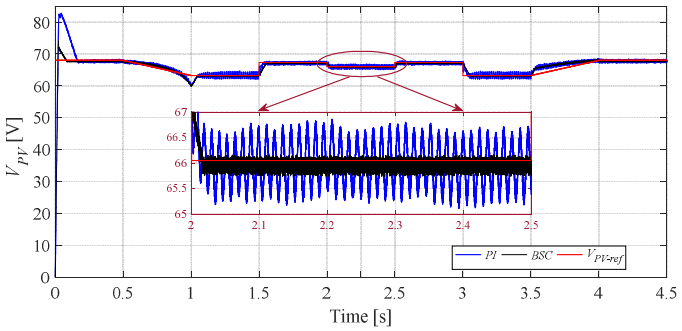

Fig. 10. Solar Panel Voltage V_{PV} with P&O/PI (blue) and P&O/BSC (black) under varying irradiance.

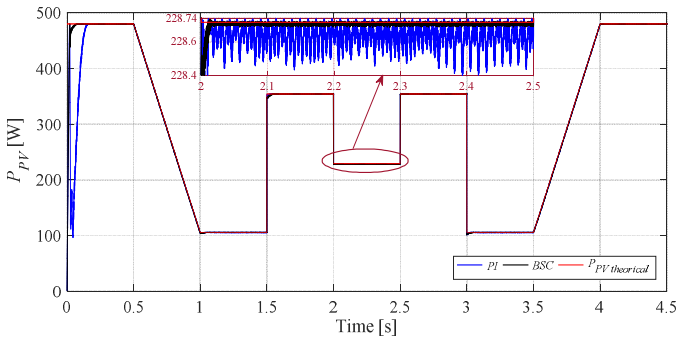

Fig. 11. P_{PV} power with P&O/PI (blue) and proposed P&O/BSC (black) under varying irradiance.

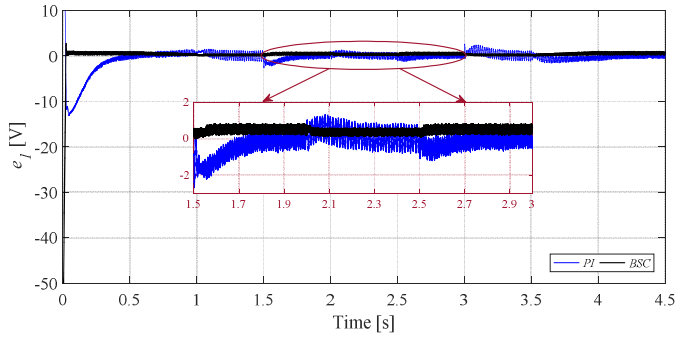

Fig. 12. Back-stepping against classical PI error signal for different solar irradiance.

Figures 10, 11 and 12 below are showing the simulation of the PV voltage (V_{PV}), PV power (P_{PV}) and error signal (e_1) with classical P&O/PI (blue) controller and the proposed P&O/BSC (black), respectively. Firstly, the irradiation level is the same to the last section. We can be seen the V_{PV} voltage with conventional PI method fluctuates around the reference $V_{PV\text{-}ref}$ in the (65.3 V - 66.67 V) range, while for the proposed BSC, the voltage range is much narrower (65.58-66.12 V).

It can be seen that the proposed P&O/BSC is able to reach in a shorter time the maximum power point than the PI. In addition the back-stepping controller results in lower maximum overshoots, response time and oscillations are very low if compared with the classical PI method.

B. Comparison under varying temperature

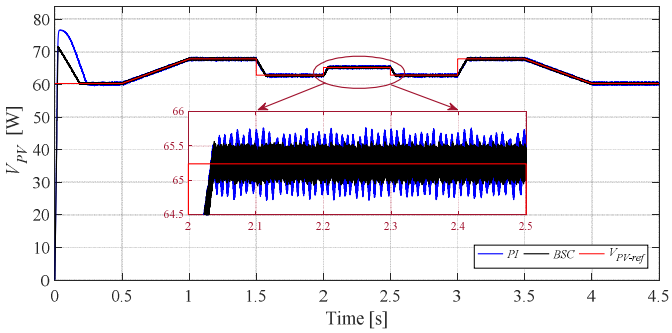

Fig. 13. V_{PV} voltage with classical P&O/PI (blue) and P&O/BSC (black) under variation temperature.

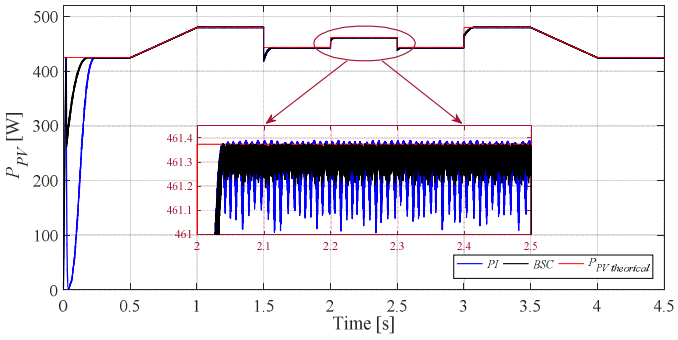

Fig. 14. Power extracted from the panel with classical P&O/PI (blue) and P&O/BSC (black) under variation temperature .

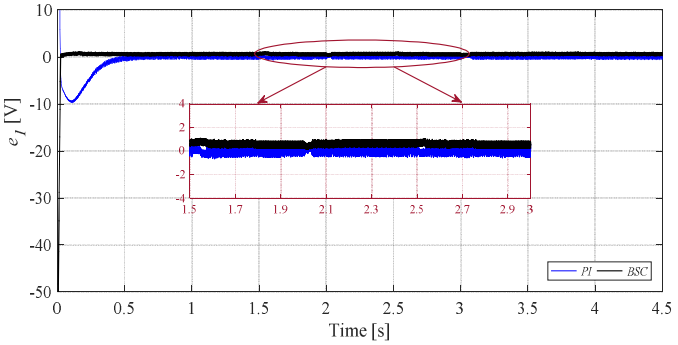

Fig. 15. Back-stepping aginst classical PI error signal for differente temperature.

Also the performance of the two different controller is studied under temperature variations.

The results are shown in Figs. 13, 14 and 15. It can be seen that the voltage V_{PV} and the power P_{PV} decrease as the temperature increase.

At steady state it can be seen that the BSC control exhibits better performance with fewer oscillations across the reference $V_{PV\text{-}ref}$ between (65 V-65.5 V) against the classical PI controller.

TABLE I. SYSTEM CHARACTERISTICS

	Parameters	***Values***
PV panel	Maximum power (*Pmpp*)	*120* W
	Open circuit voltage (*Voc*)	*42.1* V
	Short circuit current (*Isc*)	*3.86* A
	Optimum operating voltage (*Vmpp*)	*33.6* V
	Optimum operating current (*Impp*)	*3.57* A
	Cells in series (*Ns*)	*72*
	Cells in parallel (*Np*)	1
NIBB converter Components	C_1	*2200 µF*
	C_2	*1100 µF*
	L	*10 mH*
	R	*50* Ω
Back-stepping controller	K_1	*43e3*
	K_2	*100*

VI. CONCLUSION

A more efficient approach has been proposed for a fast and robust MPPT controller in PV applications. The method is based on the combination of a P&O/BSC of the optimal operating point of the PV system. The approach was compared to a classical approach consisting of a simple P&O/PI controller powered by a Perturb & Observe search algorithm found in various variations of condition for multiple mains applications . In Simulink, both approaches were implemented with a NIBB converter to validate their abilities in a real dynamic simulation, taking into account rapidly changing of climatic conditions. The analysis shows that the proposed solution is characterized by faster convergence, smaller oscillations around the equilibrium stage, and less instability and overshoot when large transients are involved.

REFERENCES

[1] A. Bahadori, C. Nwaoha, S. Zendehboudi, et G. Zahedi, « An overview of renewable energy potential and utilisation inAustralia », Renew. Sustain. Energy Rev., vol. 21, p. 582□589, mai 2013, doi: 10.1016/j.rser.2013.01.004.

[2] P. A. Owusu et S. Asumadu-Sarkodie, « A review of renewable energy sources, sustainability issues and climate change mitigation », Cogent Eng., vol. 3, no 1, p. 1167990, 2016.

[3] Y. S. Joel, H. V. Saikumar, et S. S. R. Patange, « Design & performance analysis of Fuzzy based MPPT control using two-switch non inverting Buck-Boost converter », in 2016 International Conference on Electrical Power and Energy Systems (ICEPES), 2016, p. 414–419.

[4] X Weng et al., « Comprehensive comparison and analysis of non-inverting buck boost and conventional buck boost converters », J. Eng., vol. 2019, no 16, p. 3030–3034, 2019.

[5] A. Reatti, F. Corti, A. Tesi, A. Torlai and M. K. Kazimierczuk, "Effect of Parasitic Components on Dynamic Performance of Power Stages of DC-DC PWM Buck and Boost Converters in CCM," *2019 IEEE International Symposium on Circuits and Systems (ISCAS)*, Sapporo, Japan, 2019, pp. 1-5, doi: 10.1109/ISCAS.2019.8702520.

[6] M.G. Villalva et E. Ruppert, « Analysis and simulation of the P&O MPPT algorithm using a linearized PV array model », in Industrial Electronics, 2009. IECON'09. 35th Annual Conference of IEEE, 2009, p. 231–236.

[7] K. Ishaque, Z. Salam, et G. Lauss, « The performance of perturb and observe and incremental conductance maximum power point tracking method under dynamic weather conditions », Appl. Energy, vol. 119, p. 228–236, 2014. 7

[8] A. Laib, F. Krim, B. Talbi, A. Kihal, et H. Feroura, « Improved control for three phase dual-stage grid-connected PV systems based on predictive control strategy », J. Control Eng. Appl. Inform., vol. 20, no 3, p. 12–23, 2018. 10

[9] B. Talbi, F. Krim, T. Rekioua, A. Laib, et H. Feroura, « Design and hardware validation of modified P&O algorithm by fuzzy logic approach based on model predictive control for MPPT of PV systems », J. Renew. Sustain. Energy, vol. 9, no 4, p. 043503, 2017.11

[10] E. Bianconi et al., « Perturb and observe MPPT algorithm with a current controller based on the sliding mode », Int. J. Electr. Power Energy Syst., vol. 44, no 1, p. 346–356, 2013.12

[11] A. Belkaid, J. P. Gaubert, et A. Gherbi, « An improved sliding mode control for maximum power point tracking in photovoltaic systems », J. Control Eng. Appl. Inform., vol. 18, no 1, p. 86–94, 2016.13

[12] A. Kihal, F. Krim, B. Talbi, A. Laib, et A. Sahli, « A robust control of two-stage grid-tied PV systems employing integral sliding mode theory », Energies, vol. 11, no 10, p. 2791, 2018.14

[13] H. Al-Baidhani, M. K. Kazimierczuk, T. Salvatierra, A. Reatti and F. Corti, "Sliding-Mode Voltage Control of Dynamic Power Supply for CCM," *2019 IEEE International Symposium on Circuits and Systems (ISCAS)*, Sapporo, Japan, 2019, pp. 1-5, doi: 10.1109/ISCAS.2019.8702628.

[14] B. N. Alajmi, K. H. Ahmed, S. J. Finney, et B. W. Williams, « Fuzzy-logic-control approach of a modified hill-climbing method for maximum power point in microgrid standalone photovoltaic system », IEEE Trans. Power Electron., vol. 26, no 4, p. 1022–1030, 2011.16

[15] S. Lalouni et D. Rekioua, « Modeling and simulation of a photovoltaic system using fuzzy logic controller », in Developments in eSystems Engineering (DESE), 2009 Second International Conference on, 2009, p. 23–28.17

[16] H. K. Khalil et J. W. Grizzle, Nonlinear systems, vol. 3. Prentice hall Upper Saddle River, NJ, 2002.18

[17] O. Boutebba, S. Semcheddine, F. Krim, et B. Talbi, "Design of a Backstepping-Controlled Boost Converter for MPPT in PV Chains", in 2019 International Conference on Advanced Electrical Engineering (ICAEE), 2019, p. 1–7

[18] E. Van Dijk, J. N. Spruijt, D. M. O'sullivan, et J. B. Klaassens, « PWM-switch modeling of DC-DC converters », IEEE Trans. Power Electron., vol. 10, no 6, p. 659–665, 1995.19

[19] N. H. McClamroch, « Stability of Dynamical Systems-On the Role of Monotonic and Non-Monotonic Lyapunov Functions [Bookshelf] », IEEE Control Syst. Mag., vol. 36, no 1, p. 77–78, 2016.2